INTERNATIONAL JOURNAL OF ACTA INFORMATICA
VOLUME (2024)

MACHINE LEARNING–DRIVEN STRATEGIES FOR EFFECTIVE PILEUP SUPPRESSION

Dillep Kumar Pentyala[1], Y. P.

[1]Financial Analytics, JP Morgan Chase, UNITED STATES

ABSTRACT

Pileup is a critical challenge in modern high-energy physics experiments, particularly at high-luminosity colliders where multiple particle interactions occur simultaneously within a single detector readout. These overlapping events introduce significant noise and ambiguity, complicating the accurate reconstruction of physics objects such as jets, missing transverse energy, and vertex positions. Traditional pileup mitigation techniques rely on rule-based algorithms and handcrafted features derived from detector geometry and event-level statistics. While effective to a degree, these approaches often struggle to scale with increasing collision rates and detector complexity. Recent advances in machine learning (ML) have opened new avenues for addressing pileup by enabling data-driven, adaptive, and highly granular mitigation strategies. Machine learning models, including supervised learning algorithms, deep neural networks, and graph-based architectures, can learn complex, non-linear correlations between detector signals and underlying physical interactions. By leveraging low-level detector information, such as tracking data and calorimeter deposits, ML-based methods can more precisely distinguish between particles originating from the primary interaction and those produced by secondary pileup events. This abstract explores the application of machine learning techniques to pileup suppression, highlighting their advantages over conventional methods in terms of accuracy, robustness, and scalability. It also discusses the integration of ML models into real-time and offline data processing pipelines, along with challenges related to training data quality, model interpretability, and computational efficiency. Overall, machine learning–driven pileup mitigation represents a transformative approach that enhances signal purity and enables more precise measurements in next-generation particle physics experiments.

KEYWORDS: Assessment; Information; Communication Technology; Intervention; Dyscalculia; Web-based Tools; Mobile Apps

INTRODUCTION

The Large Hadron Collider (LHC) is worked at exceptionally high immediate radiances to accomplish the enormous measurements needed to look for outlandish Standard Model (SM) or past the SM measures just as for accuracy SM estimations. At a hadron

collider, protons are assembled in packs; as the radiance increments for axed bundle dividing, the number of protons inside each bundle impacts inelastically increments. A large portion of these inelastic impacts is delicate, with the protons dissolving into, for the most part, low-energy pions that scatter all through the locator. An average result of this sort at the LHC will contribute about 0.6 GeV/rad2 of energy. Sporadically, one set of protons inside a bundle crossing impacts head-on, creating hard (high-energy) radiation of interest. At high radiance, this hard crash, or driving vertex (LV), is constantly joined by delicate proton-proton impacts called a pileup. The information gathered so far by ATLAS, and CMS has around 20 pileup crashes for each bundle crossing all things considered $(\langle \mathrm{NPU} \rangle \sim 20)$; the information in Run 3 is relied upon to contain $\langle \mathrm{NPU} \rangle \sim 80$; and the HL-LHC in Runs 4{5 will have $\langle \mathrm{NPU} \rangle \sim 200$. Moderating the effect of this additional energy on physical observables is probably the most significant test for information investigation at the LHC.

By utilizing accuracy estimations, the charged particles coming from the pileup connections can generally be followed to impact focuses (essential vertices) different from that of the driving vertex. For sure, due to the astounding vertex goal at ATLAS and CMS, the charged molecule tracks from the pileup can be identified and removed. This is the least complex pileup expulsion strategy, called charged-hadron deduction. The test with pileup evacuation is, in this way, how to recognize unbiased radiation related to the hard impact from impartial pileup radiation. Since radiation from the pileup is genuinely uniform, it tends to be taken out overall, for instance, utilizing the fly zones procedure. The fly territories method centers around amending the general energy of collimated showers of particles known as planes. Indeed, both the ATLAS and CMS tests apply fly regions or comparable procedures to align the strength of their aircraft. Shockingly, for some estimations, for example, those including plane foundation or the full radiation designs inside the stream, eliminating the radiation on average isn't sufficient.

As opposed to aligning just the energy or net 4-force of a fly, it is feasible to right the stream's constituents. By eliminating the pileup tainting from every member, it should be possible to remake more unobtrusive stream observables. We can coarsely characterize constituent pileup moderation procedures into a few classifications: constituent preprocessing, stream/occasion preparing, subjet remedies, and constituent revisions. Preparing alludes to calculations that eliminate articles and medications portray scale factors applied to person objects. Both ATLAS and CMS perform preprocessing to the entirety of their constituents before fly grouping. For ATLAS, pileup subordinate commotion edges into clustering stifle low energy calorimeter stores typical for a pileup. In CMS, charged-hadron deduction eliminates the entirety of the pileup molecule flow applicants. Stream preparing procedures are not intended only to

relieve pileups yet since they stop constituents or subjets in a stream (or occasion) that are delicate, and additionally, at broad points to the streaming hub, pileup particles are mainly eliminated. Unequivocally labeling and eliminating pileup subjects frequently performs equivalently to calculations without express pileup subjet expulsion. On transverse momentum, $p_{\mathrm{T}}^{\mathrm{cut}}$ picked on an occasion-by-occasion premise, so 50% of many pileups just fixes are sans radiation.

While preparing calculations to eliminate constituents and subjets, there are likewise strategies to remake the specific energy dispersion from the essential impact. One of the first such techniques presented was Jet Cleansing. Purifying works at the subject level, bunching and declustering planes to address each subjet independently dependent on its neighborhood energy data. Moreover, Cleansing adventures the way that the overall size of pileup fluctuations diminishes $\langle \mathrm{NPU} \rangle \to \infty$ with the goal that the unbiased pileup energy substance of subjets can be assessed from the charged pileup energy content. A progression of related procedures works on the actual constituents. One such strategy called PUPPI too utilizes nearby captured track data yet works at the molecule level instead of the subject level. PUPPI figures a scale factor for every molecule, using a neighborhood gauge roused by the planes without-jets worldview. In this paper, we will contrast our technique with PUPPI and SoftKiller.

In this paper, we present another way to deal with pileup expulsion dependent on AI. The fundamental thought is to see particles' energy circulation as the power of pixels in a picture. Convolutional neural organizations applied to fly images have found far-reaching applications in both classification and age. Past jet image applications have helped W-boson labeling, supported top quark identification and quark/gluon stream separation. The vast majority of these past applications were all classification assignments: extricating a solitary paired classier (quark or gluon, W stream or, on the other hand, foundation fly, and so forth) from an exceptionally related multidimensional info. The application to pileup expulsion is a more confounded relapse task, as the yield (a tidied up picture) ought to be of comparable dimensionality to the info. PUMML is among the first applications of current AI instruments to relapse issues in high-energy material science.

To apply the convolutional neural organization worldview to cleaning a picture itself, we misuse the following finders' ner precise goal with the calorimeters of ATLAS and CMS. Expanding on the utilization of multichannel contributions, we give our organization three-channel fly pictures: one channel for the charged LV particles, one medium for the charged pileup particles, and one track, at a somewhat lower goal, for the complete unbiased particles. We, at that point, request that the organization recreate the obscure picture for LV neutral particles. Consequently, our data sources resemble

Jet Cleansing yet binned into a standard network (as pictures) instead of single numbers for each subject. Further, the engineering is intended to be neighborhood (similarly as with Cleansing or PUPPI), with the rectification of a pixel just utilizing data in an area around it. The subtleties of our organization's engineering are portrayed in segment 2. Area 3 records its presentation in contrast with other cutting-edge procedures. The rest of the paper contains some heartiness checks, furthermore, a conversation in segment 6 of the difficulties and openings for this methodology.

PUMML ALGORITHM

The PUMML calculation aims to recreate the nonpartisan driving vertex radiation from the charged driving vertex, charged pileup, and complete nonpartisan data. Since nonpartisan particles don't have the following data accessible, the test is to decide what part of the total, impartial energy toward every path came from the primary vertex also, what part came from the pileup. To help this separation, we contribute to our organization the energy dissemination of charged particles, isolated into driving vertex and pileup commitments, notwithstanding the all-out nonpartisan energy distribution. A distinctive way to consolidate these observables is utilizing the multichannel pictures approach presented because of shading picture acknowledgment innovation.

We apply this AI procedure to R = 0:4 anti- kt jets. The streaming picture inputs are square matrices in pseudorapidity-azimuth (η, ϕ) space of size 0:9*0:9 fixated on the charged driving vertex cross over force (pT)- weighted centroid the stream. One could join all layers to decide the fly hub; however, the pivot decided from the charged driving vertex catches rules in light of its boss rakish goal and pileup heartiness. We utilize the accompanying three info channels:

red = the transverse momenta of all neutral particles
green = the transverse momenta of charged pileup particles
blue= transverse momenta of charged leading vertex particles.

The output of our organization is additionally a picture:

output = the cross-over momenta of unbiased driving vertex particles.

Just accused particles of pT > 500MeV were remembered for the green or blue channels. Charged particles not passing this set recreation cut were treated as though they were neutral particles. Something else, the detachment into channels, is expected to be great. No picture standardization or normalization was applied to the fly pictures, permitting the organization to utilize the generally cross-over energy scale in every pixel. To evade this issue, we play out a direct upsampling of every square pixel to 4*4 pixels of size $\Delta\eta \times \Delta\phi = 0.025 \times 0.025$ and partition every pixel esteem by 16 with the end goal that the absolute force in the picture is unaltered.

In rundown, the accompanying handling was applied to create the pileup pictures:

1. **Focus**: focus the stream picture by deciphering in (η, ϕ) , so the absolute charged driving vertex pT-weighted centroid pixel is at (η, ϕ) = (0; 0). This activity relates to pivoting and boosting along the pillar heading to focus the stream.

2. **Pixelate**: yield to a 0:9*0:9 area focused at $(\eta, \phi) = (0, 0)$. Make fly pictures from every single nonpartisan molecule's cross-over momenta, and the charged driving vertex particles, the charged pileup particles, and the impartial driving vertex particles. Pixelizations of $\Delta\eta \times \Delta\phi = 0.025 \times 0.025$ and $\Delta\eta \times \Delta\phi = 0.1 \times 0.1$ are utilized for the trusted and honest stream pictures, individually.

3. **Upsample**: upsample every impartial pixel to sixteen $\Delta\eta \times \Delta\phi = 0.025 \times 0.025$ pixels, keeping the all-out cross-over force in the picture unaltered.

The convolutional neural net engineering utilized in this examination took as info 36*36 pixels, three-channel pileup pictures. Two convolutional layers, each with ten filters of size 6*6 with 2*2 steps, were utilized after zero-cushioning the information pictures and the first convolutional layer with a 2-pixel buffer all sides. The subsequent layer's yield has a size 9 *9*10, with the 9*9 part comparing to the objective outcome's size and the ten relating to the number of filters in the subsequent layer. A third convolution layer with filter size 1*1 is utilized to project down to a 9*9*1 yield. This last 1*1 convolutional layer is a standard plan for dimensionality decrease. A rectified direct unit (ReLU) initiation work was applied at each stage. A schematic of the system and design has appeared in figure 1.

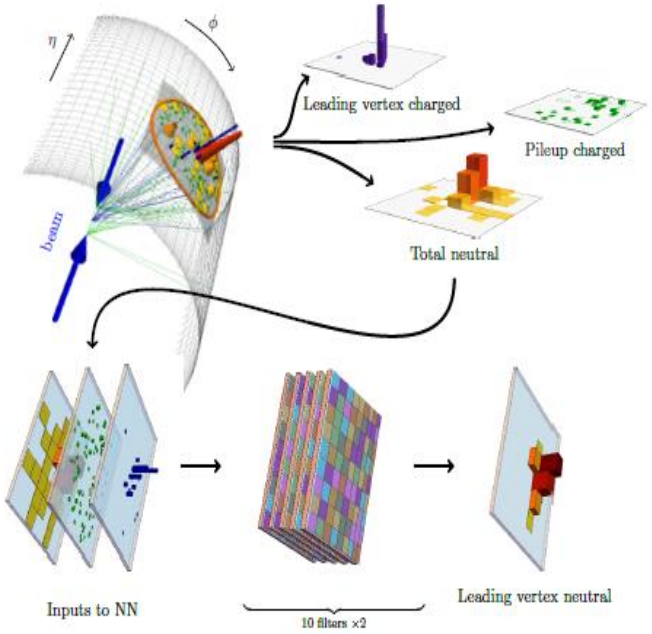

Figure 1. A representation of the PUMML structure. The info is a three-channel picture: blue/purple addresses charged radiation from the primary vertex, green is charged

pileup radiation, furthermore, yellow/orange/red is the absolute nonpartisan radiation. The goal of the captured pictures is higher than for the impartial one. These pictures are taken care of into a convolutional layer with a few filters whose esteem at every pixel is a component of a fix around that pixel area in the info pictures. The yield is a picture joining the pixels of each filter to one yield pixel.

All neural organization execution and preparation were performed with the python profound learning libraries Keras [38] and Theano [39]. The dataset comprised 56 k pileup pictures, with a 90%/10% train/test split. He-uniform introduction [40] was utilized to instate the model loads. The neural organization was prepared to use the Adam [41] calculation with a group size of 50 more than 25 ages with a learning pace of 0.001. The decision of misfortune work indeed decides an inclination for precision on more intricate pixels or gentler pixels. Keeping that in mind, the misfortune work used to prepare PUMML was a modified per-pixel logarithmic squared misfortune:

$$\ell = \left\langle \log \left(\frac{p_{\mathrm{T}}^{(\mathrm{pred})} + \bar{p}}{p_{\mathrm{T}}^{(\mathrm{true})} + \bar{p}} \right)^2 \right\rangle,$$

p is a hyperparameter that controls the decision between preferring all pT similarly (p ! 1) or preferring delicate pixels (p ! 0). After gentle advancement, an estimation of p = 10 GeV was picked. However, the model's presentation as estimated by relationships between's recreated and genuine observables is moderately robust to this decision. PUMML was found to give excellent execution even with a standard misfortune capacity, for example, the mean squared mistake, which favors all pT similarly.

This fix can be constrained by tuning the filter sizes and the number of layers in the engineering. Further, because of weight-partaking in convolutional layers, a similar capacity is applied for all pixels. Incorporating this territory and interpretation invariance into the engineering guarantees that the calculation learns a general pileup relief procedure while conveying the benefit of definitely lessening the number of model boundaries.

While we thought about planes and stream pictures in this investigation, the PUMML design utilizing convolutional nets promptly sums up to occasion-level applications. The calculation area suggests that the prepared model can be applied to any ideal location of the occasion using just the encompassing pixels. To prepare the model on the occasion level, either the current PUMML engineering could be summed up to more enormous information sources and yields. The occasion could be cut into more modest pictures, and the model prepared as in the current examination. The boundaries of the PUMML design are the convolutional filter sizes, the number of filters per layer, and the number of convolutional layers, which might be advanced for a specific application.

Here, we have introduced engineering enhanced for effortlessness and execution for fly level pileup deduction. PUMML is intended to be pertinent at both the fly and occasion levels.

PERFORMANCE

To test the PUMML calculation, we consider $q\bar{q}$ light-quark-started jets from the rot of a scalar with mass $m_\phi = 500\,\mathrm{GeV}$.. Occasions were created utilizing Pythia 8.183 with the default tune for pp crashes at $\sqrt{s} = 13\,\mathrm{TeV}$. Pileup was created by overlaying delicate QCD measures onto every occasion. Last state particles, except for muons and neutrinos, were kept. The circumstances were grouped with FastJet 3.1.3 utilizing the counter kt calculation with a fly sweep of R = 0:4. A person-level pT cut of 95 GeV was applied, and up to two driving jets $p_\mathrm{T} > 100\,\mathrm{GeV}$ and $\eta \in [-2.5, 2.5]$ were chosen from every occasion. All particles were taken to be massless.

Tests were created with the number of pileup vertices going from 0 to 180. Since the model should be prepared to fix its boundaries, the learned model relies upon the pileup dissemination utilized for preparing. For our pileup reenactments, we prepared Poisson dissemination of NPUs with mean NPU = 140. For heartiness examines, we likewise attempted preparing with NPU= 140 for every occasion or NPU= 20 for every occasion. The normal stream picture contributions for this example appear in figure 2. For examination, we show the exhibition of two incredible and generally utilized constituent-based pileup relief techniques: PUPPI, what's more, SoftKiller. In the two cases, default boundary esteems were utilized: R0 = 0:3, Rmin = 0:02, $w_\mathrm{cut} = 0.1$, $p_\mathrm{T}^\mathrm{cut}(\mathrm{NPU})$ = 0:1 + 0:007 NPU (PUPPI), framework size = 0.4 (SoftKiller). Varieties in the PUPPI boundaries didn't yield an enormous difference in execution. Both PUPPI and SoftKiller were executed at the molecule level and afterward discretized for examination with PUMML. We show the different pileup alleviation strategies on an irregular choice of occasions in figure 3. On these models, PUMML all the more effectively eliminates respectably delicate energy stores that PUPPI and SoftKiller hold. To assess the exhibition of different pileup alleviation procedures, we process a few observables and contrast the genuine qualities with the observables' rectified estimations.

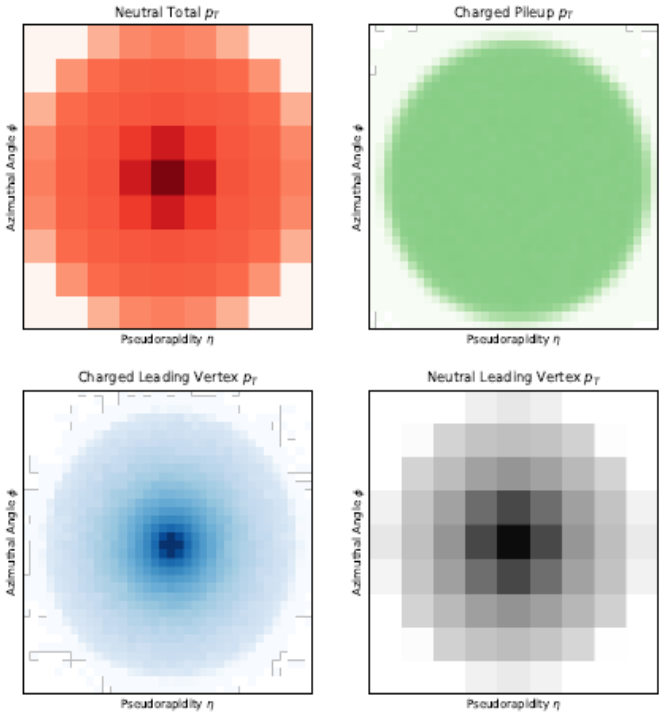

Figure 2. The average leading-jet images for a 500 GeV scalar decaying to light-quark jets with NPU = 140 pileups, separated by all neutral particles (top left), charged pileup particles (top right), charged leading vertex particles (bottom left), and neutral leading vertex particles (bottom right). The trusted and total neutral embodiments comprise the three-channel input to the neural network trained to predict the neutral ultimate vertex image.

A finder discretization is applied to the valid and reproduced occasions to encourage a correlation with PUMML, which yields remedied impartial calorimeter cells instead of arrangements of particles. Our examinations center around the accompanying six stream observables:

- Jet Mass: an invariant mass of the mainstream.
- Dijet Mass: an invariant mass of the two driving jets.
- Jet Transverse Momentum: the all-out cross-over energy of the fly.
- Neutral Image Activity N_{95} : the number of impartial calorimeter cells which account for 95% of the complete nonpartisan cross-over energy.
- Energy Correlation Functions $\mathrm{ECF}_N^{(\beta)}$: specifically, we consider the logarithm of the two-and three-point ECFs $\beta = 4$.

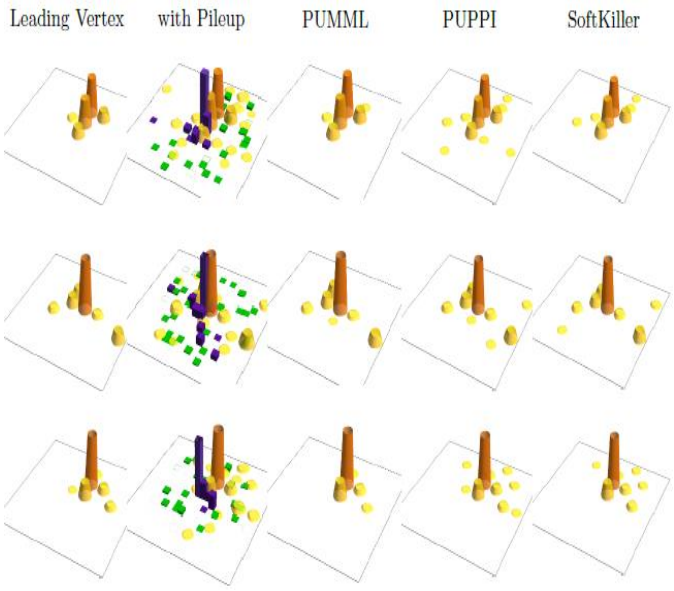

Figure 3. Depictions of three randomly chosen leading jets. Blue/purple represents charged radiation from the top vertex, green is set pileup radiation, and yellow/orange/red is the neutral radiation. Shown from left to right are the actual neutral ultimate vertex particles. The event

with pileup and charged leading vertex information, followed by the neutral ultimate vertex particles predicted by PUMML, PUPPI, and SoftKiller. From examining these events, it appears that PUMML has learned an effective pileup mitigation strategy.

Figure 4 outlines the circulations of a few of these fly observables in the wake of applying the different pileup deduction strategies. While these plots are standard, they don't give a per-occasion sign of execution. A more beneficial correlation is to show the appropriations of the per-occasion percent blunder in reproducing the genuine estimations of the observables, which are appeared in figure 5. To mathematically investigate the occasion-by-occasion effectiveness, we can look at the Pearson direct relationship coefficient between the valid and remedied values or the interquartile range (IQR) of the percent mistakes. Table 1 sums up the occasion-by-occasion connection coefficients of the conveyances that appeared in figure 4. Table 2 sums up the IQRs of the dispersions that appeared in figure 5. PUMML beats the other pileup moderation procedures on both of these measurements, with upgrades for stream-based observables, such as stream mass and energy relationship capacities.

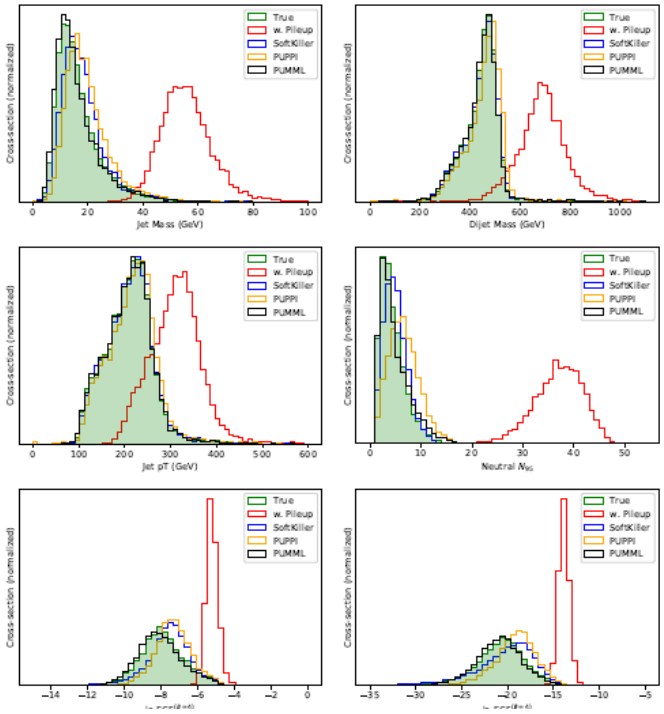

Figure 4. Distributions of leading jet mass (top left), dijet mass (top right), leading jet pT (middle left), neutral N95 (middle right), ln ECF(_=4) N=2 (bottom left), and ln ECF(_=4) N=3 (bottom right) for the considered pileup subtraction methods with Poissonian NPU = 140 pileup. While all of the pileup mitigation methods do well for observables such as the dijet mass and jet pT, PUMML more

closely matches the true distributions of more sensitive substructure observables like mass, neutral N95, and the energy correlation functions.

ROBUSTNESS

It is essential to confirm that PUMML learns a pileup moderation work that isn't excessively touchy to the NPU conveyance of its preparation test. Strength to the NPU on which it is prepared would demonstrate that PUMML is learning an all-inclusive deduction methodology. To assess this vigor, PUMML was ready on 50 k occasions with the same token NPU = 20 or NPU = 140 and afterward tried on examples with different NPUs. Figure 6 shows the stream mass relationship coefficients as an element of the test NPU. PUMML learns a methodology that is shockingly performant outside of the NPU range on which it was prepared. Further, we see that by this proportion of execution, PUMML reliably outflanks the two PUPPI and SoftKiller.

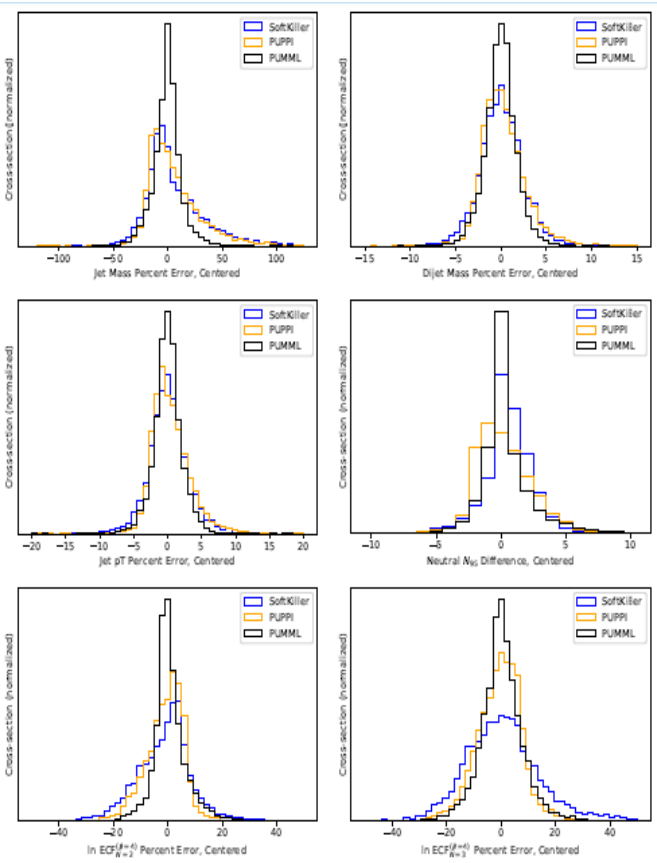

Figure 5. Distributions of the percent error between reconstructed and actual values for leading jet mass (top left), dijet mass (top right), leading jet pT (middle left), neutral N95 (middle right), ln $\mathrm{ECF}^{(\beta=4)}_{N=2}$ (bottom left), and ln $\mathrm{ECF}^{(\beta=4)}_{N=3}$ (bottom right) for the considered pileup subtraction methods with Poissonian $\langle \mathrm{NPU} \rangle = 140$ pileup. For the discrete neutral N95 observable, only the difference is shown. All distributions are centered on having a median at 0. Its taller and narrower peaks highlight the improved reconstruction performance of PUMML.

A connected robustness test is to test how the exhibition of PUMML relies upon the pT range of the preparation test. To investigate this, we created two massive preparing tests (50k occasions): one with a scalar mass of 200 GeV and one with a scalar group of 2TeV; we didn't force any parton-level pT cuts on these examples. After preparing these two organizations, we tried them on many tests produced from scalars with transitional masses, from 300 GeV to 900 GeV. The figure additionally shows that the presentation of PUMML is less touchy to of the pT of the testing test than either PUPPI or Soft-Killer. This strength test addresses the PUMML calculation's capacity to learn all-inclusive parts of pileup moderation.

Correlation (%)	w. Pileup	PUMML	PUPPI	SoftKiller
Jet mass	65.5	97.4	94.0	91.3
Dijet mass	85.5	99.5	95.8	99.1
Jet p_{T}	94.4	99.7	98.0	99.4
Neutral N_{95}	36.2	75.3	70.4	67.7
ln $\mathrm{ECF}_{N=2}^{(\beta=4)}$	60.4	90.5	83.3	68.8
ln $\mathrm{ECF}_{N=3}^{(\beta=4)}$	41.6	77.2	69.1	45.7

Table 1. Correlation coefficients between the actual and corrected values of different jet observables on an event-by-event level. The first column lists the correlation without any pileup mitigation applied to the event. More significant correlation coefficients are better.

IQR (%)	PUMML	PUPPI	SoftKiller
Jet mass	13.0	28.7	30.8
Dijet mass	2.02	2.95	2.97
Jet p_{T}	2.26	3.40	3.39
ln $\mathrm{ECF}_{N=2}^{(\beta=4)}$	5.63	8.82	11.9
ln $\mathrm{ECF}_{N=3}^{(\beta=4)}$	8.48	10.7	16.7

Table 2. The interquartile ranges (IQR) of the distributions in figure 5. Note that PUMML performs better than either PUPPI or SoftKiller. Lower IQR indicates better performance.

Various modifications of PUMML were additionally attempted. Privately associated layers were tried rather than convolutional layers. They were found to perform more terribly because of an enormous increment in the number of boundaries of the model while losing the interpretation invariance that makes PUMML incredible. We took a stab at preparing without different mixes of the information channels; the model was found to perform modestly more terribly without both of the charged media, be that as it may, endured extreme debasement without the absolute, unbiased channel. We took a stab at utilizing less complex models with just one layer or fewer filters per layer. Strikingly, even with just a solitary layer and an isolated 4 * 4 filter (a model with only 49 boundaries), PUMML performed just tolerably more awful than the form introduced in this examination, which was permitted to be more muddled to accomplish surprisingly better execution.

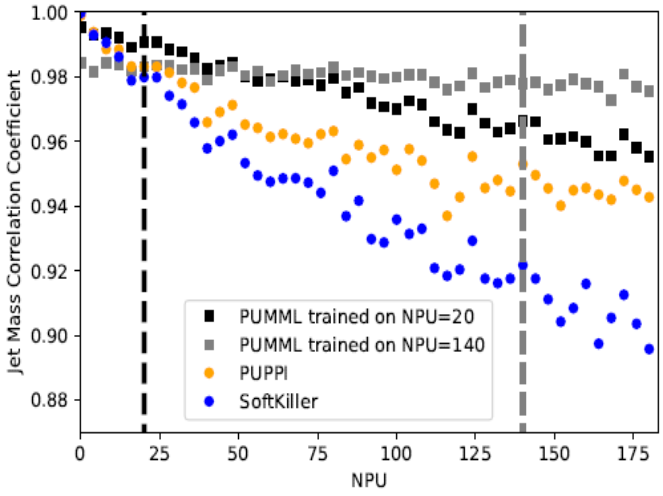

Figure 6. Correlation coefficients between reconstructed and true jet masses are plotted as NPU for the different pileup mitigation schemes. PUMML was trained on 50 k events with either NPU= 20 or NPU= 140 indicated by dashed vertical lines. The performance of PUMML with Poissonian $\langle \mathrm{NPU} \rangle = 140$ is similar to the NPU= 140 curve. PUMML is surprisingly performant well outside the NPU range on which it was trained and consistently outperforms PUPPI and SoftKiller. Note that PUMML trained on the lower NPU sample better reconstructs the jet mass

in the low pileup regime.

WHAT IS PUMML LEARNING?

While it is by and large challenging to figure out the thing an organization is learning, one potential test is to look at loads of the filter layers in the convolutional network. For our entire organization, these loads are muddled, and the subtractor that the organization learns is challenging to test systematically. We prepared a simplified PUMML network with a single 12* 12-pixel filter, which traverses 33 square pixels with no inclination term. The different channels of this filter have appeared in figure 8. The nonpartisan filter chooses the pertinent nonpartisan pixel for the deduction. The charged pileup filter is around uniform (with the worth reliant on the specific decision of misfortune capacity and actuation work), and the set driving vertex filter doesn't significantly contribute.

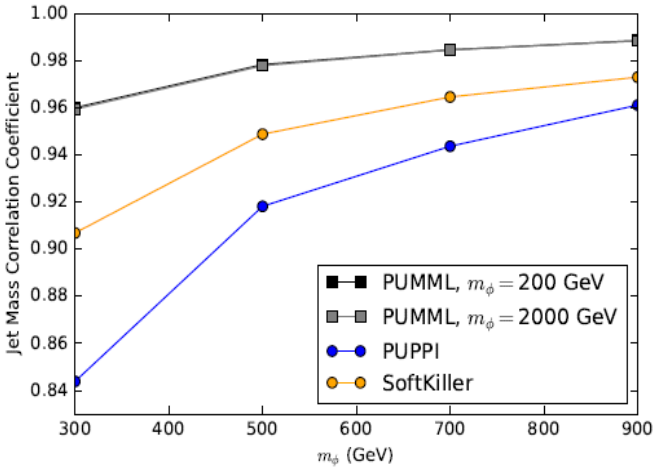

Figure 7. Correlation coe_cients between reconstructed and true jet masses are plotted as a function of the scalar resonance group with NPU=140. A spread in scalar resonances is generated to produce a range in transverse jet momenta. The two PUMML curves closely match

one another.

The filter values spur the accompanying definition of what PUMML is realizing:

$$p_{\mathrm{T}}^{\mathrm{N,LV}} = 1.0\, p_{\mathrm{T}}^{\mathrm{N,total}} - \beta\, p_{\mathrm{T}}^{\mathrm{C,PU}} + 0.0\, p_{\mathrm{T}}^{\mathrm{C,LV}}, \qquad (5.1)$$

for some, $\mathcal{O}(1)$ constant β, where $p_{\mathrm{T}}^{\mathrm{N,LV}}$, $p_{\mathrm{T}}^{\mathrm{N,total}}$, $p_{\mathrm{T}}^{\mathrm{C,PU}}$, and $p_{\mathrm{T}}^{\mathrm{C,LV}}$ are the unbiased pixel-level cross over momenta of the nonpartisan driving vertex particles, every impartial molecule, charged pileup particles, and charged driving vertex particles, separately. The qualities 1.0 and 0.0 in eq. (5.1) are steady (to the 0.05 level) under varieties in the misfortune and actuation capacities. This is consoling as the learned subtractor is subsequently influential in the $\mathrm{NPU} \to 0$ limit, notwithstanding start prepared $\langle \mathrm{NPU} \rangle = 140$.

Eq. (5.1) is strikingly like the inspired recipe utilized in Jet Cleansing. Purging is based on the perception that since pileup is the indistinguishable amount of many separate dissipating occasions, its change is more modest than the radiation from the primary vertex. Hence, it is wiser to appraise $p_{\mathrm{T}}^{\mathrm{N,PU}}$ from $p_{\mathrm{T}}^{\mathrm{C,PU}}$ than to estimate $p_{\mathrm{T}}^{\mathrm{N,LV}}$ from $p_{\mathrm{T}}^{\mathrm{C,L\bar{V}}}$. The least complex type of Cleansing (Linear Cleansing) gives the equation:

$$p_{\mathrm{T}}^{\mathrm{N,LV}} = p_{\mathrm{T}}^{\mathrm{N,tot}} - \left(\frac{1}{\overline{\gamma_0}} - 1\right) p_{\mathrm{T}}^{\mathrm{C,PU}}, \qquad (5.2)$$

where $\overline{\gamma_0}$ is the average proportion of charged pT to add up to pT in a subjet? Along these lines, this primary one 12 * 12 filter PUMML network is learning a subtractor of correctly a similar parametric structure as Linear Cleansing!

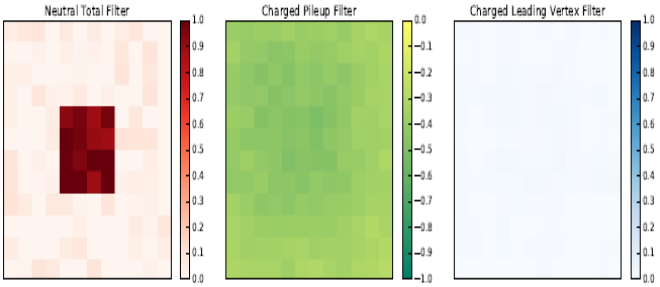

Figure 8. Filter weights for a simple PUMML network with a single 12 * 12 filter and a ReLU activation function trained with $\langle \mathrm{NPU} \rangle = 140$. The network have selected the relevant neutral pixel, turned o_ the charged leading vertex contribution, and is using the authorized pileup information

uniformly.

The estimation of $\overline{\gamma_0}$ Linear Cleansing and the assessment of that is learned in eq. (5.1) rely upon how delicate radiation is dealt with. For instance, if no remaking edge is applied $\overline{\gamma_0} \approx 2/3$ (since 2/3 of pions are charged). Likewise, the estimation of B relies upon the misfortune work utilized. For instance, if the misfortune work is limited when the methods for the valid and anticipated nonpartisan cross over momenta are equivalent:

$$\ell = \left| \langle p_{\mathrm{T}}^{(\mathrm{true})} \rangle - \langle p_{\mathrm{T}}^{(\mathrm{pred})} \rangle \right| = \left| \langle p_{\mathrm{T}}^{\mathrm{N,LV}} \rangle - \langle p_{\mathrm{T}}^{\mathrm{N,total}} \rangle + \beta \langle p_{\mathrm{T}}^{\mathrm{C,PU}} \rangle \right|, \qquad (5.3)$$

Then we find that optimal B is:

$$\beta = \frac{\langle p_{\mathrm{T}}^{\mathrm{N,PU}} \rangle}{\langle p_{\mathrm{T}}^{\mathrm{C,PU}} \rangle}. \qquad (5.4)$$

Preparing the 12*12 PUMML filter without a ReLU or predisposition term, utilizing Eq.'s misfortune work (5.3) with the normal taken pixel-wise over the group, we find B = 0:59 with no charged recreation cut and B = 1:18 with the amount. These qualities are predictable with those anticipated by eq. (5.4) of 0.62 and 1.26, individually.

Then again, if we make a mean squared blunder misfortune work:

$$\ell = \left\langle \left(p_{\mathrm{T}}^{(\mathrm{true})} - p_{\mathrm{T}}^{(\mathrm{pred})} \right)^2 \right\rangle, \qquad (5.5)$$

Then the minimum occurs at:

$$\beta = \frac{\langle p_T^{N,PU} p_T^{C,PU} \rangle}{\langle p_T^{C,PU} p_T^{C,PU} \rangle}. \qquad (5.6)$$

This relies just upon the pileup properties, likewise with Linear Cleansing, yet additionally depends on relationships among's nonpartisan and charged radiation. For instance, preparing the 12*12 PUMML filter without a ReLU or predisposition term utilizing a mean squared blunder misfortune work, we find B = 0:56 with no charged recreation cut and B = 0:97 with the amount. These numbers are in everyday understanding (inside 10{20%) with an immediate assessment of the righthand side of Eq. (5.6). In the breaking point that nonpartisan and charged pileup radiation are consistent, eq. (5.6) diminishes to eq. (5.4).

Regardless of whether the misfortune capacity of eq. (5.4) or eq. (5.6) (or something different totally) is better is not easy to build up. Incorporating the ReLU enactment work further entangles the examination since the model is similarly punished for all non-positive expectations. We find with the single 12*12 filter, utilizing the misfortune capacity of eq. (2.1) and including a ReLU and predisposition term, PUMML accomplishes a fly mass connection coefficient of 90.4%. This is serious with the qualities recorded in table 1, as we may expect since Linear Cleansing has equivalent execution to PUPPI and SoftKiller. The entire organization enhances Linear Cleansing by misusing extra connections challenging to unravel by taking a gander at the filters.

CONCLUSION

In this paper, we have presented the first use of AI to the fundamentally significant issue of pileup alleviation at hadron colliders. We have stated the case of pileup relief in the language of an AI relapse issue. The technique we presented, PUMML, takes as information the cross-over force conveyance of charged driving vertex, charged pile up, and every single impartial molecule and yields the amended driving vertex unbiased energy dissemination. We showed that PUMML works in any event too as, and regularly better than, the contending calculations PUPPI and SoftKiller in their default executions. It will be energizing to see these calculations contrasted and a full locator reproduction. It will be feasible to test the affectability to significant test effects like goals and inefficiencies.

There are a few augmentations and different uses of the PUMML system past the extent of this examination. As referenced in area 2, PUMML can generally be stretched out from fly pictures to whole occasions. Applying this occasion level PUMML to the issue of missing cross-over energy would be a following distinct stage. While the filter sizes can be something similar for the occasion and stream pictures, the organization preparing will probably require modification. Besides, the homogeneity of the locator reaction with jj will require consideration. Another possibly valuable conversion to

PUMML is to train to foresee the nonpartisan pileup pT instead of the unbiased driving vertex pT to increment the out-of-sample strength of the learned pileup alleviation calculation. Also, utilizing bigger R planes might be of interest, in this way requiring a resizing of the nearby fix or other PUMML boundaries, which is all handily accomplished.

A significant thought when utilizing AI for molecule material science applications is how the technique can be used with information and whether the deliberate vulnerabilities are leveled out. Dissimilar to a persuaded calculation, for example, PUPPI or SoftKiller, AI risks being a \black-box," which can be challenging to comprehend. In any case, AI is incredible, scalable, and able to supplement actual knowledge to take care of confounded or obstinate issues.

It is desirable to train on accurate information instead of recreation to keep the model from learning recreation relics. In many AI applications in collider material science, acquiring truth-level preparing tests in communication is a great test. To defeat this challenge in classification assignments acquaints a methodology with the train from tainted examples utilizing class extent data. For PUMML and pileup alleviation worldwide, a more straightforward strategy to prepare information is conceivable. To recreate pileup, we overlay delicate QCD occasions on top of a complex dissipating measure, both created with Pythia. Tentatively, there are enormous examples of least predisposition and zero-inclination (for instance, haphazardly set off) information. There are likewise tests of generally pileup-free occasions from low radiance runs. In this way, we can build high-pileup tests utilizing complete information. This sort of information overlay approach, which exploratory gatherings have effectively used in different settings, could be ideal for preparing PUMML with information. Consequently, execution of ML-based pileup moderation in a natural test setting could maintain a strategic distance from demonstrating curios during preparing, along these lines adding more strength and capacity to this new instrument.

REFERENCES

[1] Nayak, A., Patnaik, A., Satpathy, I., Khang, A., & Patnaik, B. C. M. (2024). Quantum Computing AI: Application of Artificial Intelligence in the Era of Quantum Computing. *In Applications and Principles of Quantum Computing* (pp. 113-128). IGI Global Scientific Publishing

[2] Putchakayala, R., & Cherukuri, R. (2022). AI-Enabled Policy-Driven Web Governance: A Full-Stack Java Framework for Privacy-Preserving Digital Ecosystems. *International Journal of Artificial Intelligence, Data Science, and Machine Learning, 3*(1), 114-123.

[3] Gudepu, B. K., & Jaladi, D. S. (2022b). Why Real-Time Data Discovery is a Game Changer for Enterprises. *International Journal of Acta Informatica, 1*(1), 164-175.

[4] Putchakayala, R., & Cherukuri, R. (2024). AI-Enhanced Event Tracking: A Collaborative Full-Stack Model for Tag Intelligence and Real-Time Data Validation. *International Journal of Artificial Intelligence, Data Science, and Machine Learning, 5*(2), 130-143.

[5] Acampora, G. (2019). Quantum machine intelligence: Launching the first journal in the area of quantum artificial intelligence. *Quantum machine intelligence, 1*(1), 1-3.

[6] Jaladi, D. S., & Vutla, S. (2024b). The Role of Artificial Intelligence in Modern Medicine. The Metascience, 2(4), 96-106

[7] Yarram, V. K., & Yallavula, R. (2022). Adaptive Machine Learning Driven Compliance Scoring Models for Automated Risk Detection, Quality Validation of AI-Generated Content in Regulated Industries. *International Journal of Emerging Research in Engineering and Technology, 3*(1), 116-126.

[8] Mattews, A., & Emma, O. (2024). The Role of Artificial Intelligence in Automating Data Governance Procedures.

[9] Yallavula, R., & Parimi, S. K. (2022). Bridging Data, Intelligence, and Trust the Future of Computational Systems and Ethical AI. *International Journal of Modern Computing, 5*(1), 119-129.

[10] Fernández Pérez, I., Prieta, F. D. L., Rodríguez-González, S., Corchado, J. M., & Prieto, J. (2022, July). Quantum AI: achievements and challenges in the interplay of quantum computing and artificial intelligence. *In International Symposium on Ambient Intelligence* (pp. 155-166). Cham: Springer International Publishing

[11] Yallavula, R., & Putchakayala, R. (2022). A Data Governance and Analytics-Enhanced Approach to Mitigating Cyber Threats in NoSQL Database Systems. *International Journal of Emerging Trends in Computer Science and Information Technology, 3*(3), 90-100.

[12] Qamar, R., Zardari, B. A., & Khang, A. (2024). Quantum Computing AI: Artificial Intelligence and Quantum Computing Applications. *In Applications and Principles of Quantum Computing* (pp. 146-161). IGI Global Scientific Publishing

[13] Cherukuri, R., & Yarram, V. K. (2024). From Intelligent Automation to Agentic AI: Engineering the Next Generation of Enterprise Systems. *International Journal of Emerging Research in Engineering and Technology, 5*(4), 142-152.

[14] Boppiniti, S. T. (2023). Data ethics in ai: Addressing challenges in machine learning and data governance for responsible data science. *International Scientific Journal for Research, 5*(5), 1-29.

[15] Yallavula, R., & Yarram, V. K. (2021). An AI Framework for Monitoring Rule Changes in Highly Volatile Compliance Environments. *The Computertech*, 39-53.

[16] Tadi, V. (2020). Optimizing data governance: Enhancing quality through AI-integrated master data management across industries. *North American Journal of Engineering Research, 1*(3).

[17] Putchakayala, R., & Yallavula, R. (2024). AI-Driven Federated Data Governance: Building Trustworthy and Sustainable Digital Ecosystems. *International Journal of Modern Computing*, *7*(1), 219-227.

[18] Parimi, S. K., & Yallavula, R. (2023). Enterprise Risk Intelligence: Machine Learning Models for Predicting Compliance, Fraud, and Operational Failures. *International Journal of Emerging Trends in Computer Science and Information Technology*, *4*(2), 173-181.

[19] Eswaran, U., Khang, A., & Eswaran, V. (2024). Role of Quantum Computing in the Era of Artificial Intelligence (AI). *In Applications and Principles of Quantum Computing* (pp. 46-68). IGI Global Scientific Publishing.

[20] Putchakayala, R., & Parimi, S. K. (2023). AI-Optimized Full-Stack Governance A Unified Model for Secure Data Flows and Real-Time Intelligence. *International Journal of Modern Computing*, *6*(1), 104-112.

[21] Pooranam, N., Surendran, D., Karthikeyan, N., Rajathi, G. I., Raj, P., Kumar, A., ... & Oswalt, M. S. (2023). Quantum computing: future of artificial intelligence and its applications. Quantum Computing and Artificial Intelligence: *Training Machine and Deep Learning Algorithms on Quantum Computers*, 163.

[22] Klusch, M., Lässig, J., Müssig, D., Macaluso, A., & Wilhelm, F. K. (2024). Quantum artificial intelligence: a brief survey. *KI-Künstliche Intelligenz*, *38*(4), 257-276.

[23] Parimi, S. K., & Yallavula, R. (2021). Data-Governed Autonomous Decisioning: AI Models for Real-Time Optimization of Enterprise Financial Journeys. *International Journal of Emerging Trends in Computer Science and Information Technology*, *2*(1), 89-102.

[24] Yarram, V. K., & Parimi, S. K. (2024). The Next Frontier of Enterprise Transformation: A Comprehensive Analysis of Generative AI as a Catalyst for Organizational Modernization, Intelligent Automation, and Large-Scale Knowledge Acceleration Across Global Digital Ecosystems. *The Metascience*, *2*(2), 97-106.

[25] Parimi, S. K., & Yarram, V. K. (2022). AI-First Enterprise Architecture: Designing Intelligent Systems for a Global Scale. *The Computertech*, 1-18.

[26] Faruk, O. M., & Sultana, M. S. (2021). Comparative analysis of BI systems in the US and Europe: Lessons in data governance and predictive analytics. *Journal of Sustainable Development and Policy*, *1*(5), 01-38.

[27] Yallavula, R., & Putchakayala, R. (2023). Governance-of-Things (GoT): A Next-Generation Framework for Ethical, Intelligent, and Autonomous Web Data Acquisition. *International Journal of Artificial Intelligence, Data Science, and Machine Learning*, *4*(4), 111-120.

[28] Gudepu, B. K., & Jaladi, D. S. (2022a). Data Discovery and Security: Protecting Sensitive Information. *International Journal of Acta Informatica*, *1*(1), 176-187.

[29] Yallavula, R., & Putchakayala, R. (2024). AI for Data Governance Analysts: A Practical Framework for Transforming Manual Controls into Automated Governance Pipelines. *International Journal of AI, BigData, Computational and Management Studies, 5*(1), 167-177.

[30] Jaladi, D. S., & Vutla, S. (2024a). Machine Learning Techniques for Analyzing Large-Scale Patient Databases. *International Journal of Modern Computing, 7*(1), 181-198.

[31] Cherukuri, R., & Putchakayala, R. (2021). Frontend-Driven Metadata Governance: A Full-Stack Architecture for High-Quality Analytics and Privacy Assurance. *International Journal of Emerging Research in Engineering and Technology, 2*(3), 95-108.

[32] Jaladi, D. S., & Vutla, S. (2023b). Revolutionizing Diagnostic Imaging: The Role of Artificial Intelligence in Modern Radiology. *The Metascience, 1*(1), 284-305.

[33] Cherukuri, R., & Putchakayala, R. (2022). Cognitive Governance for Web-Scale Systems: Hybrid AI Models for Privacy, Integrity, and Transparency in Full-Stack Applications. *International Journal of AI, BigData, Computational and Management Studies, 3*(4), 93-105.

[34] Gudepu, B. K., Jaladi, D. S., & Gellago, O. (2023). How Data Catalogs are Transforming Enterprise Data Governance: *A Systematic Literature Review. The Metascience, 1*(1), 249-264.

[35] Parimi, S. K., & Cherukuri, R. (2024). Proactive AI Systems: Engineering Intelligent Platforms that Sense, Predict, and Act. *International Journal of Emerging Trends in Computer Science and Information Technology, 5*(3), 122-130.

[36] Jaladi, D. S., & Vutla, S. (2023a). Brainy: An Intelligent Machine Learning Framework. *International Journal of Acta Informatica, 2*(1), 219-229.

[37] Cherukuri, R., & Yarram, V. K. (2023). AI-Orchestrated Frontend Systems: Neural Rendering and LLM-Augmented Engineering for Adaptive, High-Performance Web Applications. *International Journal of Emerging Research in Engineering and Technology, 4*(3), 107-114.

[38] Yarram, V. K., & Cherukuri, R. (2023). From Data to Decisions: Architecting High-Performance AI Platforms for Fortune 500 Ecosystems. *The Metascience, 1*(1), 306-324.